EBioMedicine 46 (2019) 193–201

Contents lists available at ScienceDirect

EBioMedicine

journal homepage: www.ebiomedicine.com

EBioMedicine
Published by THE LANCET

Research paper

Surprising synergy of dual translation inhibition vs. *Acinetobacter baumannii* and other multidrug-resistant bacterial pathogens

Nicholas Dillon [a], Michelle Holland [a], Hannah Tsunemoto [b], Bryan Hancock [a], Ingrid Cornax [a], Joe Pogliano [b,c], George Sakoulas [a,c,d], Victor Nizet [a,c,e,*]

[a] Department of Pediatrics, UC San Diego, La Jolla, CA 92093, USA
[b] Division of Biological Sciences, UC San Diego, La Jolla, CA 92093, USA
[c] Collaborative to Halt Antibiotic-Resistant Microbes (CHARM), UC San Diego, La Jolla, CA 92093, USA
[d] Sharp Healthcare System, San Diego, CA 92101, USA
[e] Skaggs School of Pharmacy and Pharmaceutical Sciences, UC San Diego, La Jolla, CA 92093, USA

ARTICLE INFO

Article history:
Received 9 March 2019
Received in revised form 6 July 2019
Accepted 15 July 2019
Available online 25 July 2019

Keywords:
Acinetobacter baumannii
Antibiotic therapy
Azithromycin
Minocycline
Synergy
Translation inhibition
Pneumonia
Antibiotic resistance
Bacterial cytological profiling

ABSTRACT

Background: Multidrug-resistant (MDR) *Acinetobacter baumannii* infections have high mortality rates and few treatment options. Synergistic drug combinations may improve clinical outcome and reduce further emergence of resistance in MDR pathogens. Here we show an unexpected potent synergy of two translation inhibitors against the pathogen: commonly prescribed macrolide antibiotic azithromycin (AZM), widely ignored as a treatment alternative for invasive Gram-negative pathogens, and minocycline, among the current standard-of-care agents used for *A. baumannii*.

Methods: Media-dependent activities of AZM and MIN were evaluated in minimum inhibitory concentration assays and kinetic killing curves, alone or in combination, both in standard bacteriologic media (cation-adjusted Mueller-Hinton Broth) and more physiologic tissue culture media (RPMI), with variations of bicarbonate as a physiologic buffer. Synergy was calculated by fractional inhibitory concentration index (FICI). Therapeutic benefit of combining AZM and MIN was tested in a murine model of *A. baumannii* pneumonia. AZM + MIN synergism was probed mechanistically by bacterial cytological profiling (BCP), a quantitative fluorescence microscopy technique that identifies disrupted bacterial cellular pathways on a single cell level, and real-time kinetic measurement of translation inhibition via quantitative luminescence. AZM + MIN synergism was further evaluated vs. other contemporary high priority MDR bacterial pathogens.

Findings: Although two translation inhibitors are not expected to synergize, each drug complemented kinetic deficiencies of the other, speeding the initiation and extending the duration of translation inhibition as verified by FICI, BCP and kinetic luminescence markers. In an MDR *A. baumannii* pneumonia model, AZM + MIN combination therapy decreased lung bacterial burden and enhanced survival rates. Synergy between AZM and MIN was also detected vs. MDR strains of Gram-negative *Klebsiella pneumoniae* and *Pseudomonas aeruginosa*, and the leading Gram-positive pathogen methicillin-resistant *Staphylococcus aureus*.

Interpretation: As both agents are FDA approved with excellent safety profiles, clinical investigation of AZM and MIN combination regimens may immediately be contemplated for optimal treatment of *A. baumannii* and other MDR bacterial infections in humans.

Fund: National Institutes of Health U01 AI124326 (JP, GS, VN) and U54 HD090259 (GS, VN). IC was supported by the UCSD Research Training Program for Veterinarians T32 OD017863.

1. Introduction

The emergence and spread of antibiotic resistant bacterial pathogens impose considerable morbidity and mortality on the healthcare system. As our arsenal of previously efficacious antibiotics dwindle, so too does our capacity to successfully treat patients infected with multidrug-resistant (MDR) bacterial pathogens. Among these, the Gram-negative coccobacillus *Acinetobacter baumannii* is of foremost concern in hospital-acquired infections such as ventilator-associated pneumonia, bacteremia, and urinary tract infection [1–3], and as a cause of serious wound infections among military personnel in the Iraq and Afghanistan wars [4]. *A. baumannii* is intrinsically resistant to many

* Corresponding author at: Department of Pediatrics, UC San Diego, La Jolla, CA 92093, USA.
E-mail address: vnizet@ucsd.edu (V. Nizet).

https://doi.org/10.1016/j.ebiom.2019.07.041

Research in context

Evidence before this study

Acinetobacter baumannii is a frequently multidrug-resistant (MDR) nosocomial pathogen causing pneumonia, bacteremia, and wound infections with high associated mortality rates. Among the last defenses against MDR *A. baumannii* is minocycline (MIN), which ideally would be combined in an efficacious multi-drug therapy for optimal cure rates and preservation of clinical longevity. In an earlier *eBiomedicine* study, we reported unanticipated bactericidal activity of azithromycin (AZM) in vitro and in vivo against MDR Gram-negative pathogens including *A. baumannii*, not recognized by standard antimicrobial testing paradigms. Currently, AZM is neither recommended nor utilized for serious GNR infections.

Added value of this study

AZM activity against MDR *A. baumannii* is revealed upon testing in more physiologic media (e.g. tissue culture media) and with bicarbonate present as a physiologic buffer. Although AZM and MIN are both translation inhibitors and not predicted to synergize, each drug complemented kinetic deficiencies of the other, speeding the initiation and extending the duration of translation inhibition as calculated by fractional inhibitory concentration index (FICI). Synergy of the two drugs was verified morphometrically by fluorescence-based bacterial cytological profiling and a real time assay of translation efficiency. AZM + MIN combination therapy decreased lung bacterial burden and enhanced survival rates in a murine pneumonia model, verifying in vivo relevance. AZM and MIN synergy was further documented against additional high priority MDR pathogens.

Implications of all the available evidence

Our evaluation of the best antibiotic options to treat the highest priority MDR pathogens is hamstrung by the narrowness of the current testing paradigm. Since AZM is widely prescribed and has an excellent safety profile, clinical studies adding AZM to current standard-of-care MIN could immediately be contemplated for patients suffering MDR *A. baumannii* infections, with a potential to reduce unacceptably high morbidity and mortality rates.

antibiotics and rapidly acquires additional drug resistance [5], with approximately two-thirds of hospital-acquired *A. baumannii* infections in the U.S. now classified as MDR [6]. Importantly, MDR strains of *A. baumannii* have higher associated mortality rates than drug-susceptible strains [7].

One key strategy for combating MDR pathogens is by thoughtful implementation of combination therapies, involving action on multiple targets whose combined effects increase the potency of the treatment. Multidrug therapies are predicated on drug-drug interactions instead of novel compounds, and can help reduce the evolution of resistance, since more resistance conferring adaptions are required than in monotherapy. Such therapies have been successful against a variety of difficult to treat bacterial infections (e.g. *Mycobacterium tuberculosis*) where multi-drug therapy is still efficacious despite its implementation over three decades ago [8]. Indeed, in the current era of antibiotic resistance, a number of unappreciated and underutilized drug are receiving new consideration as components of combination therapy vs. MDR pathogens [9].

Recently, we reported unanticipated bactericidal activity for azithromycin (AZM) against several MDR Gram-negative rods (GNR) including *A. baumannii*, *Klebsiella pneumoniae* and *Pseudomonas aeruginosa* that is not recognized by standard antimicrobial testing paradigms [10]. While AZM is the most commonly prescribed antibiotic in the U.S., it is not currently recommended nor utilized for serious GNR infections because of absent activity in cation-adjusted Mueller-Hinton broth (CA-MHB), the standard for antimicrobial susceptibility testing (AST) adopted by the Clinical Laboratory Standards Institute (CLSI) in the U.S. and the European Committee on AST (EUCAST). However, we recently showed AZM has excellent activity when AST is performed instead in a mammalian tissue culture type media, Roswell Park Memorial Institute 1640 media (RPMI). Furthermore, AZM synergizes strongly with host immune factors such as the cationic defense peptide cathelicidin and serum complement, or with the peptide antibiotic colistin, ultimately exerting a clear therapeutic effect in murine models of pneumonia with *A. baumannii*, *K. pneumoniae* and *P. aeruginosa* [10].

A reintroduction of AZM into the clinical arsenal to treat high-priority MDR pathogens such as *A. baumannii* will certainly involve its incorporation into combination therapy regimens. Intravenous administration of minocycline (MIN) has emerged as an important antibiotic treatment option for serious MDR *A. baumannii* infections, particularly nosocomial pneumonia, and is currently considered a standard-of-care [11,12]. While precious few antibiotics are still effective against MDR *A. baumannii*, 79.1% of clinical strains remain susceptible to MIN [13], and along with the potentially nephrotoxic colistin, MIN represents one of the last lines of defense against the pathogen. Ideally, MIN would be combined in an efficacious multi-drug therapeutic approach, thereby preserving its current activity and protecting its clinical longevity.

Despite both agents targeting the bacterial ribosome to inhibit protein synthesis at the translational level, we here report the discovery of an unexpected synergistic interaction between AZM and MIN against MDR *A. baumannii* in AST and a murine pneumonia model in vivo. The two agents exhibit different patterns of media-dependent bactericidal activity and translation inhibition kinetics that may reinforce one another to provide a rapid and sustained antibiotic effect against *A. baumannii* and other high-priority MDR pathogens.

2. Methods

2.1. Bacterial strains

Drug-sensitive *A. baumannii* strain ATCC-17978 was obtained from the American Type Culture Collection (ATCC). MDR virulent *A. baumannii* strain AB5075, isolated from a patient with tibial osteomyelitis [14], was acquired from the Walter Reed Medical Center. MDR *A. baumannii* strains GNR175J and GNR0717, as well as MDR strains of *K. pneumoniae* (K1100) and *P. aeruginosa* (P4), are all recent clinical isolates from a tertiary academic hospital in New York [10,15]. Community-acquired MRSA USA300 strain TCH1516 was isolated from an adolescent patient at Texas Children's Hospital [16]. MDR *A. baumannii* strain AB5075- luxCDABE was constructed via insertion of the Tn7-luxCDABE mini-Tn7 element (obtained from D. Zurawski, Walter Reed Army Medical Center) into the *att*Tn7 site in AB5075 by described methods [14,17].

2.2. Antibiotics

MIN (Rempex Pharmaceuticals) and AZM (Fresenius Kabi) were purchased from a clinical pharmacy and resuspended in 1× Dulbecco's phosphate-buffered saline (DPBS) (Corning). Concentrated stocks of AZM were prepared at 100 mg/ml and MIN at 20 mg/ml. Fresh 10× or 20× experimental stocks of AZM and MIN were made in 1× DPBS at the desired concentration prior to the start of each experiment.

2.3. Reagents and bacterial culturing conditions

Bacterial strains for antibiotic susceptibility testing were first streaked on LB agar (LA) plates from stocks stored at −80 °C (in 20%

glycerol/80% MHB) and grown to stationary phase at 37 °C overnight. Isolated colonies were picked from the plate and inoculated into 5 ml of either CA-MHB (MHB (Difco) supplemented with 20 μg/ml Ca^{2+} and 10 μg/ml Mg^{2+}) or RPMI+ (phenol free RPMI (Gibco 1640) + 10% LB (Criterion)) media in a 14 ml Falcon polypropylene round-bottom snap cap tube (Corning #352059) and grown shaking at 100 rpm overnight at 37 °C. The following day, overnight cultures were sub-cultured 1:50 in the desired medium and volume in either 14 ml snap cap tubes or 50 ml polypropylene conical tubes (Corning #352098) and grown shaking at 100 rpm at 37 °C until mid-logarithmic phase (~OD_{600} = 0.4). Unless otherwise noted, experiments were conducted in Costar flat-bottom 96 well plates (Corning #3370) with a final volume of 200 μl/well.

2.4. MIC determination

Bacteria were cultured in the same media throughout (CA-MHB or RPMI+) prior to the addition of antibiotics. Mid-logarithmic phase cultures were diluted to approximately 5×10^5 CFU (~OD_{600} = 0.002) and 180 μl added to each experimental well of a 96 well flat bottom plate. Either 20 μl of 1xDPBS or 20 μl of the desired 10× drug stock were added to each well. Plates were incubated shaking at 100 rpm at 37 °C overnight. Bacterial growth (OD_{600}) was determined approximately 20 h later with an Enspire Alpha multimode plate reader (PerkinElmer). To calculate the MIC_{90}, defined as the amount of drug required to inhibit ≥90% of the growth of the untreated controls, the density of each drug-treated well was compared to untreated control. Determination of synergy was performed in the same manner except combinations of AZM and MIN were examined using checkerboard assays, where 10 μl from 20× stocks of each drug were added to each well so that the ratio of media to drugs remained consistent to the monotherapy MIC experiments. Fractional inhibition concentrations (FIC) were determined for each drug in combination and a fractional inhibition concentration index (FICI) value was calculated. Synergy was defined as an FICI value ≤0.5 [18].

2.5. Bactericidal activity assays

A. baumannii AB5075 was cultured in CA-MHB for both the overnight and the next day mid-logarithmic cultures. The latter was used to inoculate 15 ml of either CA-MHB, RPMI+, or 80% RPMI +20% fresh human whole blood with approximately 5×10^5 CFU (~OD_{600} = 0.002). The venous blood was collected in small samples from healthy volunteers under a simple phlebotomy protocol approved by the University of California, San Diego (UCSD) Institutional Review Board. Each experimental well of the 96-well flat bottom plate received 180 μl of bacterial culture and 20 μl of the desired 10× drug stock. Plates were incubated shaking at 100 rpm at 37 °C overnight. After 20 h, plates were removed from the incubator and serial 10-fold dilutions of each well performed in CA-MHB. Twenty microlitres of each serial dilution was spot plated onto LA and incubated at 37 °C overnight to enumerate the CFU.

2.6. Mouse pneumonia model

All animal experiments were conducted under veterinary supervision and approved by the UCSD IACUC. *A. baumannii* AB5075 was grown in CA-MHB as described for the bactericidal activity experiments. Mid-logarithmic phase cultures were centrifuged at 3202 xg, supernatant removed, and pellets resuspended and washed in an equal volume of 1×DPBS three times, before the final pellet was resuspended in 1× DPBS to yield a culture of 2.5×10^9 CFU/ml.

For in vivo studies, all mice were housed in an SPF barrier facility on a 12/12 light/dark cycle in Innovive Innocage pre-bedded corn cob disposable cages on a 2020× diet from Envigo. Mice were randomized at least 48 h prior to infection by the UCSD vivarium staff (blind to the researcher) into groups of 5 mice for the survival studies; additional groups of 2–3 randomized mice were added for lung enumeration studies. No more than 5 mice were housed within the same cage and no cage contained mice from different groups. No differences in the relevant health statuses of the groups were present prior to the infection and no unexpected adverse events occurred beyond lethargy and mortality due to the infections. All animals were included in the analysis.

Forty microlitres of the resuspended culture was used to intratracheally infect 8-week-old juvenile female C57Bl/6 J mice (Jackson Labs) under 100 mg/kg ketamine (Koetis) + 10 mg/kg xylazine (VetOne) anesthesia using an operating otoscope (Welch Allyn) between 2 and 4 PM PT as previously described [10]. Post-infection, mice were allowed to recover on a sloped heated pad and then returned to their home cage. At 1 h and 24 h post-infection, the mice were treated with 100 μl of either AZM (sub-cutaneous injection) or MIN (inter-peritoneal injection) at the desired drug concentrations. AZM and MIN doses were reconstituted in 1× DPBS (Corning) and pre-loaded into 1 cc U-100 insulin syringes (Becton Dickinson). For survival experiments, mice were monitored for a total of 6 days. Surviving mice were euthanized at 6 days post-infection through CO_2 exposure followed by cervical dislocation. For lung CFU enumeration studies, mice were euthanized 30 h post-infection under the same euthanasia procedure, all 5 lung lobes removed, and the tissues placed into a 2 ml sterile microtube (Sarstedt) containing 1 mm silica beads (Biospec) and 1 ml 1×DPBS. The tissue samples were homogenized for 1 min on a MagNA Lyser (Roche), followed by 1 min on ice x 3, then 10-fold serially diluted, plated on LA plates, and grown and incubated overnight for CFU determination.

2.7. Bacterial cytological profiling

Fluorescence microscopy was performed as previously described [19] with modifications. In brief, AB5075 was grown in CA-MHB or RPMI+ at 37 °C to a starting OD_{600} ~0.13 and then treated with appropriate concentrations of MIN, AZM, or combination of both antibiotics for 2 h at 37 °C. After treatment, cells were stained with 10 μg/ml FM4-64, 4 μg/ml DAPI, and 0.5 μM SYTOX-Green. Samples were transferred to a glass slide containing an agarose pad (1.2% agarose in 20% CA-MHB or RPMI+) for microscopy. Image analysis was done using FIJI (ImageJ 1.51w).

2.8. Translational activity assays

Strain AB5075-luxCDABE contains the full luciferase cassette and is therefore capable of constituently producing both the enzyme and substrate required for luminescence. AB5075-luxCDABE was cultured in either CA-MHB or RPMI+ as described for the MIC determination experiments. As in the MIC experiments, 180 μl of an approximately 5×10^5 CFU (~OD_{600} = 0.002) culture was added to each experimental well of a 96-well plate containing 20 μl of the 10× stock of the desired drug, or 10 μl of a 20× stock of each drug for AZM + MIN combination experiments. Plates were incubated stationary at 37 °C and sampled hourly for 13 h. At each timepoint, the Enspire Alpha multimode plate reader (PerkinElmer) was used to sequentially measure both the luminescence and OD_{600} of each well. To control for alterations in luminescence due to cellular density changes the total luminescent signal was divided by the OD_{600} value of the culture within each well. For the AZM + MIN combination experiments the luminescence/OD_{600} values for each well were divided by the value obtained for the untreated control wells to calculate the percent translational activity of each data point. A line of additivity was calculated for the combination treatment by combining the percent change in translation activity of each drug in monotherapy. Combination values which fell below the line of additivity were considered to have a synergistic interaction.

2.9. Statistics

All statistical analysis was conducted in GraphPad prism 7. A two-way ANOVA was utilized to determine significant effects due to treatment with AZM and/or MIN where indicated. Tukey's multiple comparison test was used to determine significant differences between treatment groups. Statistical significance was defined as p value <.0500 with * ≤0.0500–0.0100, ** ≤0.0100–0.0010, *** ≤0.0010–0.0001, and **** ≤0.0001.

3. Results

3.1. AZM and MIN show reciprocal media-dependent inhibitory activities vs. MDR A. baumannii

Minimum inhibitory concentrations (MIC) of MIN and AZM against *A. baumannii* were determined in (a) a standard rich bacteriologic testing medium (cation-adjusted Mueller-Hinton broth, CA-MHB), or (b) the common tissue culture medium RPMI, which contains the physiological buffer bicarbonate anion (HCO_3-). To ensure bacterial growth equivalency to CA-MHB, RPMI was supplemented with 10% Luria broth (LB), hereafter designated RMPI+. Four *A. baumannii* strains were examined: antibiotic-sensitive laboratory standard ATCC17978 and MDR clinical isolates AB5075, GNR175J and GNR0717. As shown in Table 1, AZM had negligible activity against all four *A. baumannii* strains in standard CA-MHB (MIC_{90} 32 to 128 μg/ml), but potent activity against the bacteria in RPMI+ (MIC 0.25 to 2 μg/ml). Conversely, MIN had strong activity against all four strains in standard CA-MHB (MIC_{90} 0.25 to 4 μg/ml) yet lost all activity against the bacteria in RPMI+ (MIC_{90} ≥ 256 μg/ml) (Table 1). Focusing on MDR *A. baumannii* strain AB5075, we quantified bacterial colony-forming units (CFU) to ascertain bactericidal activity. In CA-MHB (Fig. 1A and B), MIN showed potent killing activity (MBC_{99} = 1 μg/ml) whereas AZM was ineffective (MBC_{99} > 32 μg/μl); conversely in RPMI+ (Fig. 1D and E), AZM was highly bactericidal (MBC_{99} = 2.5 μg/ml) while MIN was completely inactive (MBC_{99} > 64 μg/ml). Similar results were seen when RPMI was supplemented with 20% freshly isolated human blood instead of 10% LB (Fig. 1G and H), with complete killing of *A. baumannii* by AZM at 1 μg/ml, but only partial killing of the bacterium at high MIN concentrations of 8 to 64 μg/ml.

3.2. AZM and MIN combinations have synergistic activity vs. MDR A. baumannii

Both MIN and AZM are bona fide bacterial translation inhibitors, with MIN (like other tetracyclines) binding to the 30S ribosomal subunit to block binding of aminoacyl-tRNA to the mRNA-ribosome complex [20], and AZM (like other macrolides) binding to the 50S subunit to obstruct the nascent peptide exit tunnel and reshape the bacterial proteome [21]. The independent binding targets of the two drugs and the discordant media dependent activity profiles led us to explore the utility of combining both drugs to develop a condition-independent regimen for targeting translation in MDR *A. baumannii*. Indeed, used in combination, MIN and AZM interacted synergistically, as defined by a fractional inhibitory concentration index (FICI) of ≤0.5 [18] in both test media: CA-MHB (Fig. 1C, FICI = 0.38) and RPMI+ (Fig. 1F, FICI = 0.09). Combinations of AZM and MIN were also found to have synergistic bactericidal activity in 20% human blood, as measured via a fractional bactericidal concentration index (FBCI, [22]) of ≤0.5 (Fig. 1I, FBCI = 0.50).

Table 1
Minimum inhibitory concentration (MIC) testing of *Acinetobacter baumannii* strains in standard bacteriologic media cation-adjusted Meuller-Hinton broth (CA-MHB) vs. tissue culture Roswell Park Memorial Institute (RPMI) media supplemented with 10% Luria broth.

MIC_{90} (μg/ml) in MHB-CA and RPMI + 10% LB				
	CA-MHB		RPMI + 10% LB	
	AZM	MIN	AZM	MIN
Acinetobacter baumannii				
ATCC-17978	64–128	0.25	0.5	≥256
AB5075 (MDR)	128	1	0.25	≥256
GNR175J (MDR)	32–64	4	1–2	≥256
GNR0717 (MDR)	128	2	0.25	≥256

3.3. Media-dependent antibiotic activity of MIN and AZM is influenced by bicarbonate

We hypothesized the opposing media-dependent antibiotic activity profiles of MIN and AZM vs. *A. baumannii* could involve a differential response to HCO_3– present in the tissue culture media but absent in the bacteriological media. We therefore titrated $NaHCO_3$ into bicarbonate-free RPMI+ medium to assess its impact on the activity of both AZM and MIN. Increasing the concentration of $NaHCO_3$ led to a marked reduction in the AZM MIC while simultaneously increasing the MIN MIC (Fig. 2A). When the concentration of each drug was held constant (MIN 2 μg/ml and AZM 1 μg/ml), a threshold level of 12 mM $NaHCO_3$ led to a dramatic increase in AZM bactericidal activity (Fig. 2B) while abolishing MIN bactericidal activity (Fig. 2C), a pattern maintained through the physiological HCO_3- serum concentration of ~24 mM.

3.4. Therapeutic benefit of combined AZM and MIN in a murine model of A. baumannii pneumonia

Having identified potent synergy between AZM and MIN in vitro, we moved to assess the in vivo efficacy of adding AZM to MIN in a murine *A. baumannii* pneumonia model. Adult C57BL/6 mice were infected intratracheally with a lethal challenge dose of MDR *A. baumannii* AB5075 and treated 1 h and 24 h post infection with varying doses of AZM and MIN. The AZM dosages in mice were selected to approximate that used in human patients, with the maximum 50 mg/kg AZM in mice recapitulating the recommended 500–1000 mg patient dose [23]. Two concentrations of MIN were chosen that did not exceed the standard 200–400 mg daily dose limit in humans (6 mg/kg) [11,24,25]. The first dose was chosen to be ineffective as monotherapy (0.39 mg/kg), conferring no reductions in lung bacterial burden (Fig. 3A) nor survival advantage with 100% mortality (Fig. 3B). The second MIN dose of 0.78 mg/kg was chosen to be suboptimal as monotherapy, with no changes in lung bacterial burdens (Fig. 3A) but providing an 80% survival rate (Fig. 3C). AZM doses of 12.5, 25, 50 mg/kg alone had no effect on the lung bacterial burdens (Fig. 3A), and even at the highest dose of 50 mg/kg provided no survival advantage (Fig. 3B and C). However, mice that received AZM in addition to the previously ineffective MIN dose of 0.39 mg/kg showed a dose-dependent reduction in their lung bacterial loads (Fig. 3A), and a clear survival advantage with a survival rate increase from 0% with either drug alone to 80% when 50 mg/kg AZM was used in combination with MIN treatment (Fig. 3B). Adding AZM to 0.78 mg/kg MIN significantly reduced lung bacterial loads in a dose-dependent fashion (Fig. 3A) while also increasing the survival rate of the MIN-treated mice from 80% to 100% at the highest (50 mg/kg) AZM dose (Fig. 3C).

3.5. Bacterial cytological profiling (BCP) demonstrates augmented translation inhibition in MDR A. baumannii upon AZM plus MIN cotreatment

To further explore the synergistic interaction between AZM and MIN, we employed BCP, a powerful technique that uses quantitative fluorescence microscopy to identify disrupted bacterial cellular pathways on a single cell level [19]. A characteristic signature of translation inhibition evident in BCP is formation of DNA toroids that arise due to changes in chromosome compaction when ribosome activity is disrupted [19]. In

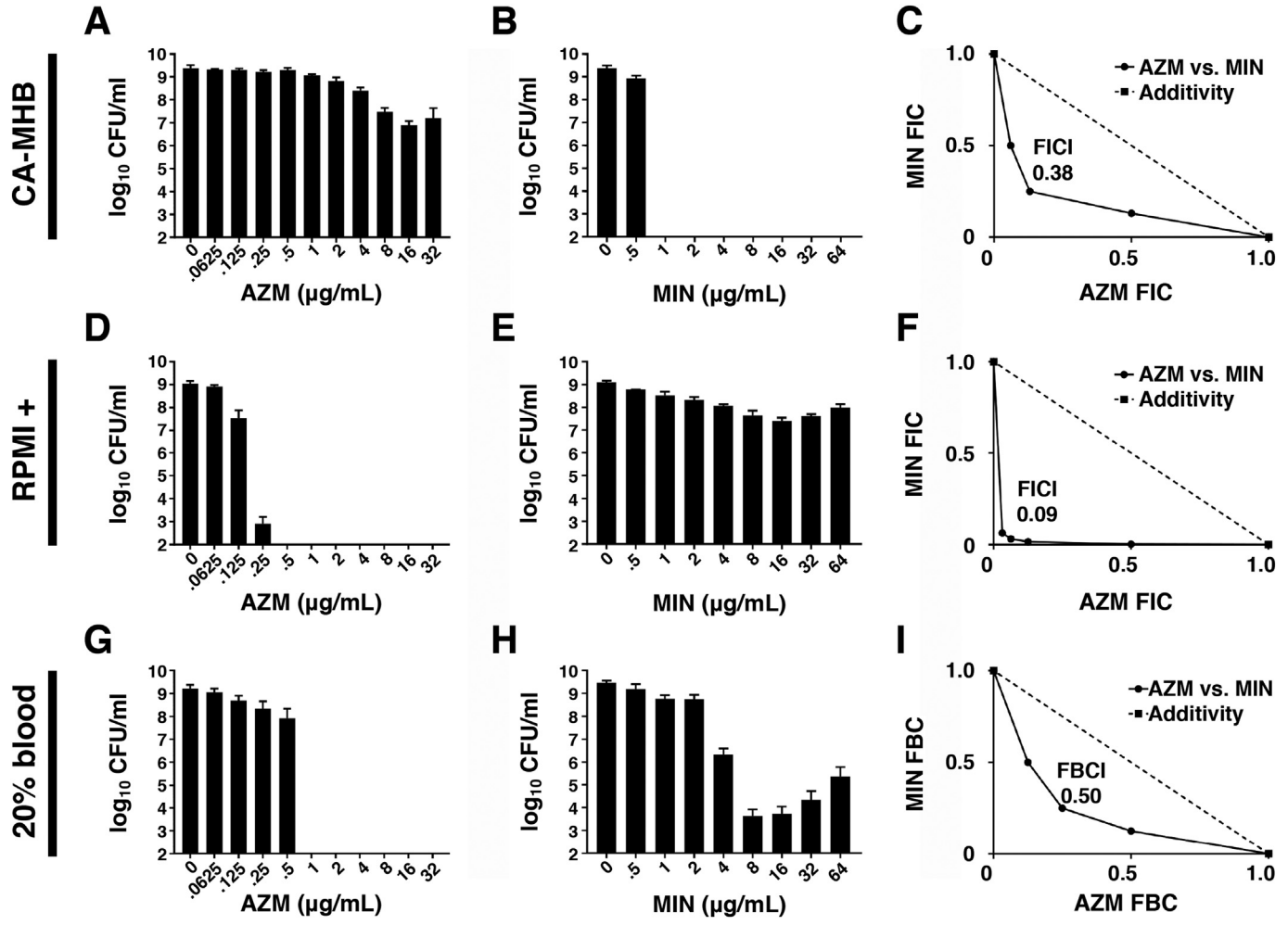

Fig. 1. AZM and MIN show reciprocal media-dependent inhibitory activities vs. MDR *A baumannii* and synergize strongly when combined. AZM and MIN activities were assessed in the standard bacteriological medium CA-MHB (*A-C*), in the physiologically relevant amended tissue culture medium RPMI+ (*D-F*), and in the presence of 20% fresh human whole blood (*G-I*). *(A)* Bactericidal activity of AZM in CA-MHB. *(B)* Bactericidal activity of MIN in CA-MHB. *(C)* Fractional inhibition concentration (FIC) plot for AZM and MIN combinations in CA-MHB. *(D)* Bactericidal activity of AZM in RPMI+. *(E)* Bactericidal activity of MIN in RPMI+. *(F)* FIC plot for AZM and MIN combinations in RPMI+. *(G)* Bactericidal activity of AZM in 20% fresh human whole blood/ 80% RPMI. *(H)* Bactericidal activity of MIN in 20% fresh human whole blood/ 80% RPMI. *(I)* Fractional bactericidal concentration (FBC) plot for AZM and MIN combinations in 20% fresh human whole blood/ 80% RPMI. All experiments were conducted in triplicate. A representative plot is shown for each of the fractional inhibition/ bactericidal graphs. Synergy is indicated by an FICI or FBCI of ≤0.5.

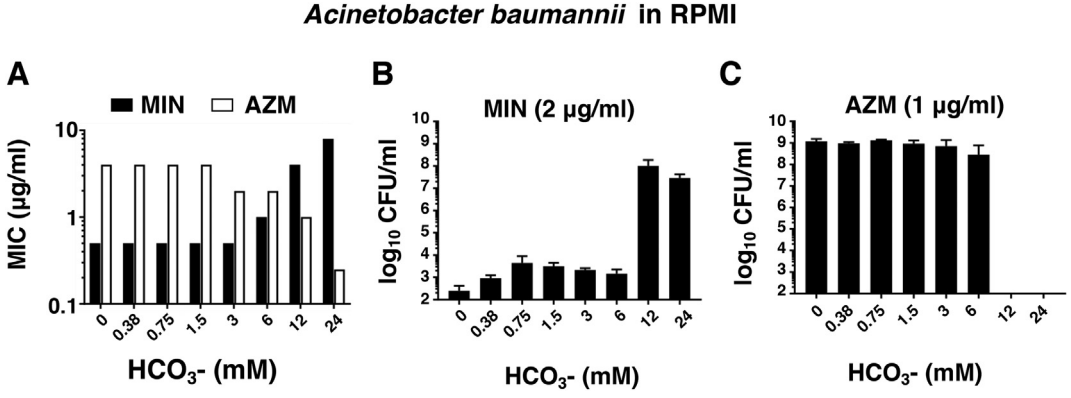

Fig. 2. Media-dependent antibiotic activity of MIN and AZM is influenced by bicarbonate. *(A)* MIC of AZM or MIN required to inhibit 90% of the untreated controls in HCO_3- free medium amended with various concentrations of HCO3-. *(B)* Bactericidal activity of 2 μg/ml of MIN in HCO_3- free medium amended with various concentrations of HCO_3-. *(C)* Bactericidal activity of 1 μg/ml of AZM in HCO_3- free medium amended with various concentrations of HCO_3-. All experiments were conducted in triplicate.

both CA-MHB and RPMI+, we identified drug concentrations in which neither AZM nor MIN inhibited *MDR A. baumannii* translation on their own, as confirmed by minimal toroid formation (Fig. 4A and C). Extensive toroid formation was observed, however, when the two drugs were co-administered at these same concentrations (Fig. 4A and C). In CA-MHB, visible toroids were seen in 2.2% of untreated

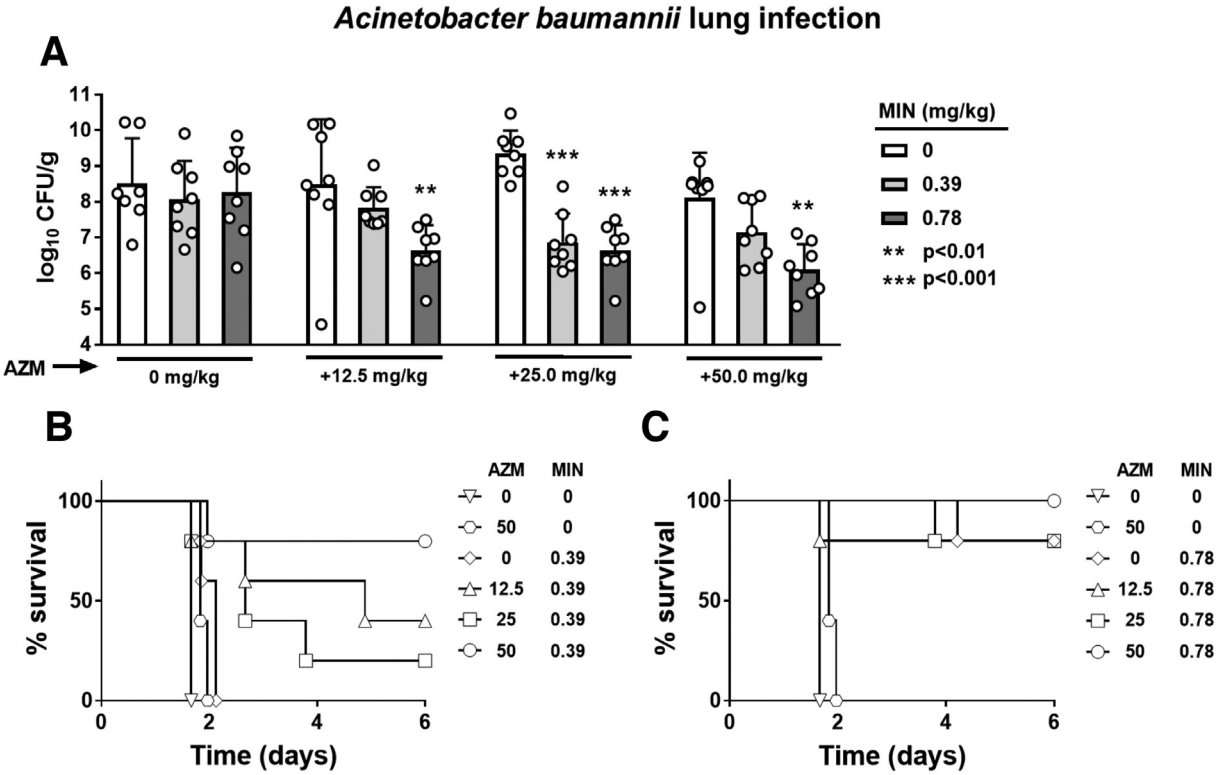

Fig. 3. Therapeutic benefit of AZM and MIN combinations in a murine model of *A. baumannii* pneumonia. C57BL/6J mice were infected intratracheally with 1×10^8 MDR *A. baumannii* strain AB5075. AZM and MIN were administered subcutaneously and intraperitoneal respectfully, both 1 and 24 h post infection at the indicated dosages. *(A)* Lungs were harvested 30 h post infection, homogenized, and plated for CFU enumeration. $N = 7$ for the no drug controls and $n = 8$ for each treatment condition. *(B)* and *(C)* Mouse survival was monitored for 6 days with $n = 5$ animals per group. For panels *(A)*, statistical significance was calculated using a two-way ANOVA with ** ≤0.01 and *** ≤0.001, interactions are considered non-significant unless otherwise noted.

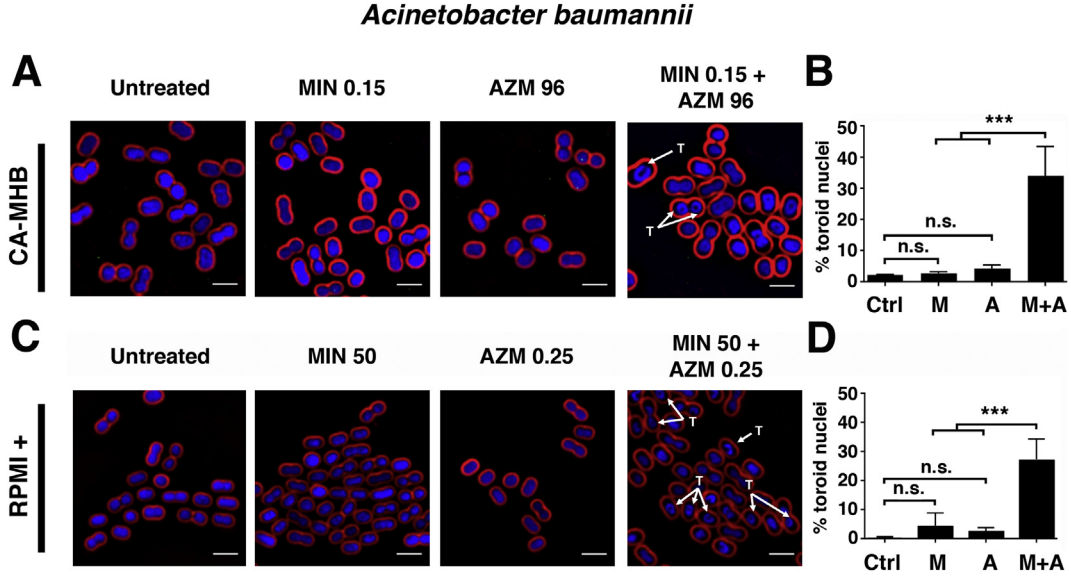

Fig. 4. Bacterial cytological profiling (BCP) demonstrates augmented translation inhibition in MDR *A. baumannii* upon AZM + MIN cotreatment. *A. baumannii* strain AB5075 cells were grown in CA-MHB to a starting OD_{600} of 0.13 and treated for 2 h with MIN, AZM, or both drugs combined. Cells were strained for fluorescence microscopy with FM4–64 (red cell membrane dye), DAPI (blue DNA dye), and SYTOX-Green (green membrane-impermeable DNA dye, used as proxy for cell lysis). "T" denotes observed toroidal nuclei. *(A)* BCP was carried out for AZM and MIN both alone and in combination in CA-MHB. *(B)* The percentage of total cells counted, between 100 and 200 in at least 3 frames, with toroid nuclei for untreated and treated cultures in CA-MHB. *(C)* BCP was carried out for AZM and MIN both alone and in combination in RPMI+. *(D)* The percentage of total cells counted, between 100 and 200 in at least 3 frames, with toroid nuclei for untreated and treated cultures in RPMI+. BCP images are representative of 3 independent experiments. Percent total toroid containing cells is combined data from 3 independent experiments for each media type. Scale bar = 2 μm. For panels *(B)* and *(D)*, statistical significance was calculated using a two-way ANOVA with ** ≤0.01 and *** ≤0.001.

A. baumannii cells, 2.8% of cells treatment with 0.15 μg/ml MIN, 4.2% of cells treated with 96 μg/ml AZM, and 34.0% of cells treated with 0.15 μg/ml MIN + 96 μg/ml AZM (Fig. 4B). In RPMI+, visible toroids were seen in 0.3% of untreated *A. baumannii* cells, 4.5% of cells treatment with 50 μg/ml MIN, 2.5% of cells treated with 0.25 μg/ml AZM, and 27.2% of cells treated with 50 μg/ml MIN + 0.25 μg/ml AZM (Fig. 4D).

3.6. Nonoverlapping translation inhibition kinetics underlie AZM and MIN synergy vs. MDR A. baumannii

To better understand the dynamics of AZM and MIN translational inhibition synergy, we employed a reporter derivative of MDR *A. baumannii* (AB5075-luxCDBAE) that contains the full luciferase cassette and can independently synthesize both enzyme and substrate needed for luminescence. Intrinsic luminescence is lost upon translational inhibition as synthesis of the required components is blocked, and drug treatment effects can be determined kinetically on a cellular level as the ratio of luminescence signal per optical density (OD_{600}), thus controlling for bacterial replication. When used alone in CA-MHB, AZM-induced translation inhibition in *A. baumannii* was delayed, allowing for initial bacterial growth, but sustained once inhibition occurred throughout the remaining course of the experiment (Fig. 5A). The late onset of AZM-associated translation inhibition, and its subsequent long-lasting effects, were even more pronounced in RPMI+, where sub-MIC concentrations of 1/4 and 1/2 the AZM MIC eventually inhibited *A. baumannii* translation despite allowing initial transcription and growth (Fig. 5D). Conversely, MIN was found to robustly inhibit translation in CA-MHB even at sub-MIC concentrations (Fig. 5B), but this inhibition was short-lived, and at concentrations of 1/16 and 1/8 the MIC, translation soon resumed (Fig. 5B). The fast-acting but short-lived translational inhibition by MIN was even more pronounced in RPMI+, where concentrations of 1/64, 1/32 and 1/16 the MIC all permitted protein synthesis after initial inhibition (Fig. 5E). To analyze the value of combining MIN + AZM against MDR *A. baumannii*, we calculated percent luminescence compared to untreated control at each time point. At sub-MIC concentrations for the individual drugs, combinations of MIN + AZM were both fast-acting and long-lasting compared to single drug treatments in both CA-MHB (Fig. 5C) and RPMI+ (Fig. 5F) media. Generating a line of additivity by combining the change in percent inhibition of each drug alone, MIN + AZM combination therapy surpassed the additive effects of the single drug treatments in both media conditions (Fig. 5C and F).

3.7. AZM and MIN synergy against additional high-priority MDR bacterial pathogens

Having established clear synergism of AZM + MIN dual therapy vs. MDR *A. baumannii*, we examined the combination potential against other high priority MDR human pathogens: Gram-negative *P. aeruginosa* and *K. pneumoniae* and Gram-positive methicillin-resistant *Staphylococcus aureus* (MRSA). As seen with *A. baumannii*, media-dependent conditional antibiotic activities of MIN (CA-MHB potency ≫ RPMI+ potency) and AZM (RPMI+ potency ≫ CA-MHB potency) were confirmed for all three additional species (Table 2). For the Gram-negative pathogens, strong synergy was observed vs. MDR *K. pneumonia* in both CA-MHB (Fig. 6A, FICI = 0.38) and RPMI+10%LB (Fig. 6D, FICI = 0.19) while synergy against MDR *P. aeruginosa* was identified only in CA-MHB (Fig. 6B, FICI = 0.50) and fell short in RPMI + (Fig. 6E, FICI = 0.53). Of note, the two drugs synergized against MDR *S. aureus* in both CA-MHB (Fig. 6C, FICI = 0.31) and RPMI+ (Fig. 6F, FICI = 0.38) indicating AZM + MIN synergy is not restricted to Gram-negative pathogens. Future studies are required to confirm that such broad-spectrum synergy of AZM and MIN extends to in-vivo infection models.

4. Discussion

Under ideal circumstances, antimicrobial therapy would sufficiently reduce bacterial burden at the end of therapy to reduce the likelihood of relapse and the emergence of drug resistance. Therapies with conditionally independent activity profiles are desirable because efficient bacterial killing in vivo typically requires eliminating the pathogen from multiple host microenvironments. On their own, both AZM and MIN

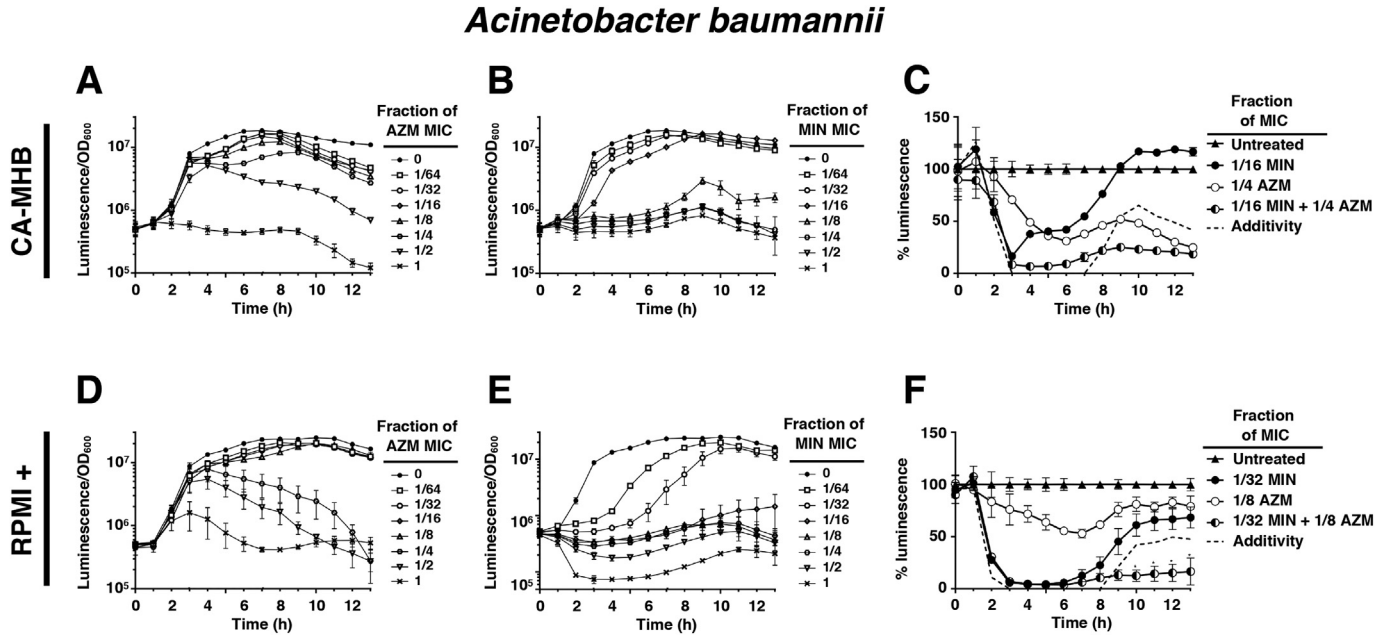

Fig. 5. Nonoverlapping translation inhibition kinetics underlie AZM and MIN synergy vs. MDR *A. baumannii*. To assess translational activity on a cellular level independent of the bacterial concentration the ratio between the luminescence and cellular density, as measured by OD_{600}, was calculated. Drug concentrations are represented as the fraction of the MIC for each drug in monotherapy at that respective condition. *(A)* Translation inhibitory activity of AZM in CA-MHB. *(B)* Translation inhibitory activity of MIN in CA-MHB. *(C)* Translational inhibition activity of AZM and MIN combination therapy, as compared to the same concentration of each drug in monotherapy, in CA-MHB. Data is presented as a percentage of the untreated control. The dashed line indicates the calculated activity expected from combining the measured activity of each drug in monotherapy. *(D)* Translation inhibitory activity of AZM in RPMI+. *(E)* Translation inhibitory activity of MIN in RPMI+. *(F)* Translational inhibition activity of AZM and MIN combination therapy, as compared to the same concentration of each drug in monotherapy, in RPMI+. Data is presented as a percentage of the untreated control. The dashed line indicates the calculated activity expected from combining the measured activity of each drug in monotherapy. All experiments were conducted in triplicate and their results were averaged. For panels (*A, B, D* and *E*) error bars were calculated using the standard deviation at each point. For panels (*C* and *F*) statistical significance was calculated using a two-way ANOVA with * ≤0.05 and ** ≤0.01.

Table 2
Minimum inhibitory concentration (MIC) testing of multidrug-resistant (MDR) bacterial strains in standard bacteriologic media cation-adjusted Meuller-Hinton broth (CA-MHB) vs. tissue culture Roswell Park Memorial Institute (RPMI) media supplemented with 10% Luria broth.

MIC_{90} (μg/ml) in MHB-CA and RPMI +10% LB				
	CA-MHB		RPMI + 10% LB	
	AZM	MIN	AZM	MIN
Klebsiella pneumoniae – K1100 (MDR)	16	8	1	≥256
Pseudomonas aeruginosa – P4 (MDR)	8–16	16	2	≥256
Staphylococcus aureus – TCH1516 (MDR)	1000	0.125	0.25–0.5	4–8

displayed media-dependent conditional activity, a potential limiting trait for their use in monotherapy. However, AZM + MIN combination therapy complemented the intrinsic inhibition profile seen with either drug alone, yielding a conditionally-independent synergistic therapy with efficacy against MDR *A. baumannii* in laboratory culture and a murine pneumonia model. The synergistic drug combination promoted enhanced translation inhibition kinetics, melding the fast-acting activity of MIN with the sustained inhibition of AZM to create a potent, long-lasting, and efficacious antibiotic profile.

The AZM + MIN drug-drug interaction appears to represent a parallel pathway interaction, when the two drugs, often each having suboptimal activity against the same primary target, combine their activities to more effectively inhibit a bacterial system or biochemical pathway [26–28], in this case protein translation at the ribosome. Both drugs have associated deficiencies as monotherapy. AZM activity is notably delayed due to its slow release from tissues [29] and a low rate of association with ribosomes [30]. Compared to AZM, the therapeutic window for MIN is shorter (half-life ~ 12–16 h in humans) [31] and its bactericidal capacity has been brought into question [32,33]. In combination, however, expedited MIN activity buys time for the slower acting, yet longer lasting, AZM-associated inhibition to occur. Furthermore, the media-dependent activity of each drug was complemented by the other, so that their synergistic activity was independent of media composition. And while we established parallel pathway synergy for MIN + AZM in translation inhibition kinetics, an important caveat of our study is that we cannot exclude the possibility of additional mechanisms of synergy such as compounding downstream effects on a tertiary target, or one drug acting to improve the bioavailability of the other [26–28].

This study also highlights the benefit of investigating antibiotic activity in more than one medium condition to infer potential clinical efficacy and opportunities for synergistic therapy. Limitations of testing only the standard bacteriological medium (CA-MHB) have previously been illustrated [10,34], testing in a more physiologic tissue culture-based medium was also not fully predicative of in vivo efficacy as MIN is active in the murine pneumonia model despite little to no activity in RPMI+. One important compositional difference between the two media we have highlighted is the presence of the physiological buffer bicarbonate anion (HCO_3-) in RPMI. HCO_3- is an essential component of multiple biological processes in humans and its presence stimulates both transcriptional and translational changes in bacteria [35], impacting antibiotic activity against numerous species when added to CA-MHB [34]. Recent work has linked HCO_3- mediated effects on antibiotic activity to reductions in bacterial proton motive force [36]. While AZM activity is known to improve in response to a loss of proton motive force, indicating that AZM is not actively imported [37], the entry of tetracyclines into the bacterial cell is an energy dependent process requiring active transport [38]. Enhanced macrolide activity against both *Escherichia coli* and *Staphylococcus aureus* have been reported in the presence of HCO_3- due to the dissipation of the pH gradient required for a functioning proton motive force [34]. The loss of active transport renders the bacteria unable to export AZM leading to its intracellular accumulation, an effect which has previously been associated with enhanced AZM activity [10].

In summary, the therapeutic potential of AZM and MIN combination therapy warrants clinical study as the two drugs were found to interact synergistically against MDR *A. baumannii* in all conditions and models examined in this study. This benefit may extend to other MDR pathogens, in particular MDR *K. pneumoniae* and MRSA. A limitation of our study at present is that future work is required to explore if MIN synergy is also found with other macrolides. Nevertheless, as both AZM and MIN

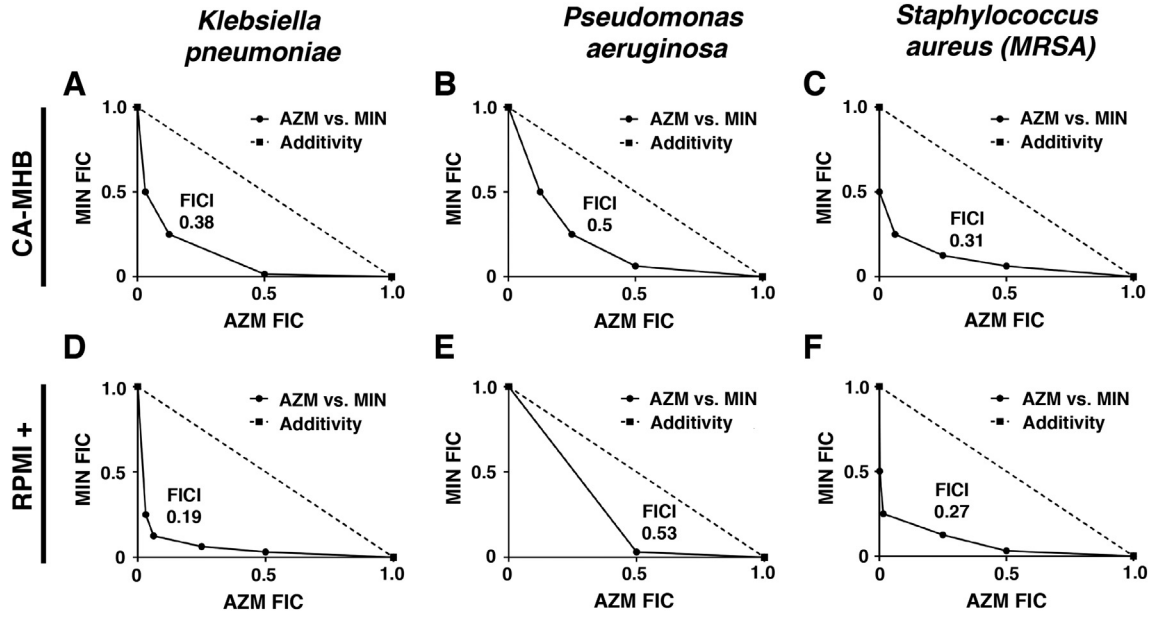

Fig. 6. AZM and MIN synergy against additional high-priority MDR pathogens. AZM and MIN synergy experiments were conducted against other important MDR human pathogens utilizing checkerboard assays. All data are presented as fractional inhibition concentration plots where the MIC of each drug in monotherapy is set to 1.0. *(A)* MDR *K. pneumoniae* strain K1100 in CA-MHB. *(B)* MDR *P. aeruginosa* strain P4 in CA-MHB. **(C)** MDR *S. aureus* strain TCH1516 in CA-MHB. *(D)* MDR *K. pneumoniae* strain K1100 in RPMI+. *(E)* MDR *P. aeruginosa* strain P4 in RPMI+. *(F)* MDR *S. aureus* strain TCH1516 in RPMI+. A representative plot is shown for each experiment that was conducted in triplicate. The FICI is indicated on the graph with an FICI of ≤0.5 indicating synergistic interactions.

are already FDA approved, readily available for use, and familiar to clinicians, the potential for clinical trials to determine the efficacy of the combinatorial therapy for *A. baumannii* is immediately at hand.

Author contributions

Drs. Dillon and Nizet had full access to all of the data in the study and take responsibility for the integrity of the data and the accuracy of data analysis.

Study concept and design: Dillon, Sakoulas, Nizet.

Acquisition, analysis or interpretation of data: All authors.

Laboratory experiments: Dillon, Holland, Tsunemoto, Hancock.

Drafting of manuscript: Dillon, Nizet.

Administrative, technical or material support: Tsunemoto, Pogliano.

Statistical analysis: Dillon, Cornax.

Critical revision of the manuscript for important intellectual content: All authors.

Declaration of Competing Interests

Dr. Pogliano owns stock in and receives consulting fees from Linnaeus Bioscience Inc. outside the submitted work. Dr. Sakoulas reports personal fees from The Medicines Company/Melinta Therapeutics, outside the submitted work. Dr. Nizet reports other from Cellics Therapeutics, grants and other from InhibRx, grants, personal fees and other from Cidara Therapeutics, personal fees from Iogen, Inc., personal fees from SutroVax, other from Centauri Therapeutics, all outside the submitted work. ND, MH, HT, BH and IC have no conflicts to disclose.

Funding/support

This is research was funded by the National Institutes of Health U01 AI124326 (JP, GS, VN) and U54 HD090259 (GS, VN). IC was supported by the UCSD Research Training Program for Veterinarians T32 OD017863.

Role of the funder/sponsor

The Funders had no role in the design and conduct of the study; collection, management, analysis, and interpretation of the data; preparation, review, or approval of the manuscript; and decision to submit the manuscript for publication.

References

[1] McConnell MJ, Actis L, Pachon J. Acinetobacter baumannii: human infections, factors contributing to pathogenesis and animal models. FEMS Microbiol Rev 2013;37(2):130–55.
[2] Ong CW, Lye DC, Khoo KL, Chua GS, Yeoh SF, Leo YS, et al. Severe community-acquired *Acinetobacter baumannii* pneumonia: an emerging highly lethal infectious disease in the Asia-Pacific. Respirolo 2009;14(8):1200–5.
[3] Dijkshoorn L, Nemec A, Seifert H. An increasing threat in hospitals: multidrug-resistant *Acinetobacter baumannii*. Nat Rev Microbiol 2007;5(12):939–51.
[4] O'Shea MK. Acinetobacter in modern warfare. Int J Antimicrob Agents 2012;39(5):363–75.
[5] Perez F, Hujer AM, Hujer KM, Decker BK, Rather PN, Bonomo RA. Global challenge of multidrug-resistant *Acinetobacter baumannii*. Antimicrob Agents Chemother 2007;51(10):3471–84.
[6] Centers for Disease Control and Prevention. Antibiotic resistance threats in the United States. US Department of Health and Human Services; 2013.
[7] Lee HY, Chen CL, Wu SR, Huang CW, Chiu CH. Risk factors and outcome analysis of acinetobacter baumannii complex bacteremia in critical patients. Crit Care Med 2014;42(5):1081–8.
[8] Floyd K. Global tuberculosis report 2016. WHO Report; 2016.
[9] Talbot GH, Bradley J, Edwards Jr JE, Gilbert D, Scheld M, Bartlett JG, et al. Bad bugs need drugs: an update on the development pipeline from the antimicrobial availability task force of the Infectious Diseases Society of America. Clin Infect Dis 2006;42(5):657–68.
[10] Lin L, Nonejuie P, Munguia J, Hollands A, Olson J, Dam Q, et al. Azithromycin synergizes with cationic antimicrobial peptides to exert bactericidal and therapeutic activity against highly multidrug-resistant gram-negative bacterial pathogens. EBioMed 2015;2(7):690–8.
[11] Ritchie DJ, Garavaglia-Wilson A. A review of intravenous minocycline for treatment of multidrug-resistant *Acinetobacter* infections. Clin Infect Dis 2014;59(Suppl. 6):S374–80.
[12] Lashinsky JN, Henig O, Pogue JM, Kaye KS. Minocycline for the treatment of multidrug and extensively drug-resistant *A. baumannii*: a review. Infect Dis Ther 2017;6(2):199–211.
[13] Castanheira M, Mendes RE, Jones RN. Update on *Acinetobacter* species: mechanisms of antimicrobial resistance and contemporary in vitro activity of minocycline and other treatment options. Clin Infect Dis 2014;59(Suppl. 6):S367–73.
[14] Jacobs AC, Thompson MG, Black CC, Kessler JL, Clark LP, McQueary CN, et al. AB5075, a highly virulent isolate of *Acinetobacter baumannii*, as a model strain for the evaluation of pathogenesis and antimicrobial treatments. MBio 2014;5(3):14–e01076.
[15] Fair RJ, Hensler ME, Thienphrapa W, Dam QN, Nizet V, Tor Y. Selectively guanidinylated aminoglycosides as antibiotics. ChemMedChem 2012;7(7):1237–44.
[16] Gonzalez BE, Martinez-Aguilar G, Hulten KG, Hammerman WA, Coss-Bu J, Avalos-Mishaan A, et al. Severe staphylococcal sepsis in adolescents in the era of community-acquired methicillin-resistant *Staphylococcus aureus*. Pediatrics 2005;115(3):642–8.
[17] Kumar A, Dalton C, Cortez-Cordova J, Schweizer HP. Mini-Tn7 vectors as genetic tools for single copy gene cloning in *Acinetobacter baumannii*. J Microbiol Methods 2010;82(3):296–300.
[18] Odds FC. Synergy, antagonism, and what the chequerboard puts between them. J Antimicrob Chemother 2003;52(1):1.
[19] Nonejuie P, Burkart M, Pogliano K, Pogliano J. Bacterial cytological profiling rapidly identifies the cellular pathways targeted by antibacterial molecules. Proc Natl Acad Sci U S A 2013;110(40):16169–74.
[20] Chukwudi CU. rRNA binding sites and the molecular mechanism of action of the tetracyclines. Antimicrob Agents Chemother 2016;60(8):4433–41.
[21] Kannan K, Vazquez-Laslop N, Mankin AS. Selective protein synthesis by ribosomes with a drug-obstructed exit tunnel. Cell 2012;151(3):508–20.
[22] Hallander HO, Dornbusch K, Gezelius L, Jacobson K, Karlsson I. Synergism between aminoglycosides and cephalosporins with antipseudomonal activity: interaction index and killing curve method. Antimicrob Agents Chemother 1982;22(5):743–52.
[23] Beigelman A, Gunsten S, Mikols CL, Vidavsky I, Cannon CL, Brody SL, et al. Azithromycin attenuates airway inflammation in a noninfectious mouse model of allergic asthma. Chest 2009;136(2):498–506.
[24] Agwuh KN, MacGowan A. Pharmacokinetics and pharmacodynamics of the tetracyclines including glycylcyclines. J Antimicrob Chemother 2006;58(2):256–65.
[25] Bowers DR, Cao H, Zhou J, Ledesma KR, Sun D, Lomovskaya O, et al. Assessment of minocycline and polymyxin B combination against *Acinetobacter baumannii*. Antimicrob Agents Chemother 2015;59(5):2720–5.
[26] Zimmermann GR, Lehar J, Keith CT. Multi-target therapeutics: when the whole is greater than the sum of the parts. Drug Discov Today 2007;12(1–2):34–42.
[27] Yeh PJ, Hegreness MJ, Aiden AP, Kishony R. Drug interactions and the evolution of antibiotic resistance. Nat Rev Microbiol 2009;7(6):460–6.
[28] Wambaugh MA, Shakya VPS, Lewis AJ, Mulvey MA, Brown JCS. High-throughput identification and rational design of synergistic small-molecule pairs for combating and bypassing antibiotic resistance. PLoS Biol 2017;15(6):e2001644.
[29] Lode H. The pharmacokinetics of azithromycin and their clinical significance. Eur J Clin Microbiol 1991;10(10):807–12.
[30] Dinos GP, Michelinaki M, Kalpaxis DL. Insights into the mechanism of azithromycin interaction with an Escherichia coli functional ribosomal complex. Mol Pharmacol 2001;59(6):1441–5.
[31] Shankar C, Nabarro LEB, Anandan S, Veeraraghavan B. Minocycline and tigecycline: what is their role in the treatment of carbapenem-resistant gram-negative organisms? Microb Drug Resist 2017;23(4):437–46.
[32] Tang HJ, Chen CC, Ko WC, Yu WL, Chiang SR, Chuang YC. In vitro efficacy of antimicrobial agents against high-inoculum or biofilm-embedded meticillin-resistant *Staphylococcus aureus* with vancomycin minimal inhibitory concentrations equal to 2 mug/mL (VA2-MRSA). Int J Antimicrob Agents 2011;38(1):46–51.
[33] Yang YS, Lee Y, Tseng KC, Huang WC, Chuang MF, Kuo SC, et al. In vivo and in vitro efficacy of minocycline-based combination therapy for minocycline-resistant *Acinetobacter baumannii*. Antimicrob Agents Chemother 2016;60(7):4047–54.
[34] Ersoy SC, Heithoff DM, Lt Barnes, Tripp GK, House JK, Marth JD, et al. Correcting a fundamental flaw in the paradigm for antimicrobial susceptibility testing. EBioMedicine 2017;20:173–81.
[35] Dorschner RA, Lopez-Garcia B, Peschel A, Kraus D, Morikawa K, Nizet V, et al. The mammalian ionic environment dictates microbial susceptibility to antimicrobial defense peptides. FASEB J 2006;20(1):35–42.
[36] Farha MA, French S, Stokes JM, Brown ED. Bicarbonate alters bacterial susceptibility to antibiotics by targeting the proton motive force. ACS Infect Dis 2018;4(3):382–90.
[37] Capobianco JO, Goldman RC. Erythromycin and azithromycin transport into *Haemophilus influenzae* ATCC-19418 under conditions of depressed proton motive force (Delta-mu-H). Antimicrob Agents Chemother 1990;34(9):1787–91.
[38] Yamaguchi A, Shiina Y, Fujihira E, Sawai T, Noguchi N, Sasatsu M. The tetracycline efflux protein encoded by the Tet(K) gene from *Staphylococcus aureus* is a metal-tetracycline/H+ antiporter. FEBS Lett 1995;365(2–3):193–7.